Revista Internacional de Investigación e Innovación Tecnológica

Página principal: www.riiit.com.mx

Walnut shell for removal by adsorption of methylene blue from aqueous solution

Cáscara de nuez para la remoción por absorción de azul de metileno en solución acuosa

Puente-Luna, L.I.[a], Arévalo-Niño, K.[a], Lara-Banda, M.R.[b], Rojas-Verde, G.[a], Almaguer-Cantú, V.[a]*

[a] Universidad Autónoma de Nuevo León, Facultad de Ciencias Biológicas, Instituto de Biotecnología. Av. Pedro de Alba y Manuel L. Barragán s/n, 66455. San Nicolás de los Garza, Nuevo León, México.
[b] Universidad Autónoma de Nuevo León, Facultad de Ingeniería Mecánica y Eléctrica, Laboratorio de Análisis de Falla, Centro de Investigación e Innovación en Ingeniería Aeronáutica. Carr. a Salinas Victoria, 65582 Aeropuerto del Nte., Nuevo León, México.
laura.puenteln@uanl.edu.mx; katiushka.arevalonn@uanl.mx; maria.laraba@uanl.edu.mx: guadalupe.rojasvrd@uanl.edu.mx; veronica.almaguerct@uanl.edu.mx*

Technological innovation: Agricultural waste is ecological and sustainable and can be attractive to be used for pollutants as an environmental field.

Industrial application area: Textile industries could also consider the use of this type of materials that come from natural origin with absorbent properties to treat their effluents before being discarded into the environment; this could be something positive and sustainable for this type of industries.

Received: november 11th, 2024
Accepted: march 06th, 2025

Resumen

Se utilizó cáscara de nuez (CN) como material adsorbente agrícola para eliminar el azul de metileno (AM) de soluciones acuosas y se evaluó en un proceso discontinuo. CN se analizó mediante microscopía electrónica de barrido (MEB) e infrarrojo por transformadas de Fourier (IR-TF). Los experimentos se realizaron dependiendo del tiempo de contacto, la dosis de adsorbente (0,5 y 0,1 g), la agitación (50 y 100 rpm) y la temperatura (293 y 313 K), concentración inicial del adsorbato (50 mg/L). Los datos cinéticos se analizaron utilizando ecuaciones de pseudo primer y pseudo segundo orden. Los datos isotérmicos se modelaron con las ecuaciones de Langmuir y Freundlich. Los datos de la isoterma de adsorción encajan bien con la isoterma de Langmuir y se encontró que la capacidad de adsorción de la monocapa era de 80,65 mg/g para AM. La adsorción de AM en CN se confirma mediante IRTF y MEB. El estudio termodinámico revela que la adsorción de AM en CN se realiza mediante una reacción endotérmica (ΔH = 1.097 kJ/mol), factible y espontánea (ΔG^0

= -21,157.32 kJ/mol a 293 K; -23,363.13 kJ/mol a 303 K; y -17,333.87 kJ/mol a 313 K) y disminuye el desorden de las moléculas. En el proceso de adsorción (ΔS^0 = -2,63 kJ/mol K). La eficiencia del CN en AM estuvo relacionada con la disposición de los sitios de adsorción, así como con la estructura microporosa del material adsorbente. Los resultados indicaron que la cáscara de nuez podría ser una alternativa a los adsorbentes más caros que se utilizan para eliminar este colorante.

Palabras clave: Azul de metileno, Cáscara de nuez, Cinética, Equilibrio, Isoterma de adsorción.

Abstract

Walnut shells (WS) were used as an agricultural adsorbent material to remove methylene blue (MB) from aqueous solutions and evaluated in a batch process. WS was analyzed by Scanning Electron Microscopy (SEM) and Fourier transform infrared (FTIR). The experiments were carried out depending on the contact time, the dose of adsorbent (0.5 and 0.1 g), the agitation (50 and 100 rpm) and the temperature (293 and 313 K), initial concentration of the adsorbate (50 mg/L). The kinetic data were analyzed using pseudo-first order and pseudo-second order equations. Isotherm data were modeled with the Langmuir and Freundlich equations. The adsorption isotherm data fit well with the Langmuir isotherm and the adsorption capacity of the monolayer was found to be 80.65 mg/g for MB. MB adsorption on WS is confirmed by FTIR and SEM. The thermodynamic study reveals that MB adsorption in WS is carried out by an endothermic reaction (ΔH = 1,097 kJ/mol), feasible and spontaneous (ΔG^0 = -21,157.32 kJ/mol a 293 K; -23,363.13 kJ/mol a 303 K; y -17,333.87 kJ/mol a 313 K) and decreases the disorder of the molecules in the adsorption process (ΔS^0 = –2.63 kJ/mol K). The efficiency of the WS on MB was related to the arrangement of adsorption sites, as well as the microporous structure of the adsorbent material. The results indicated that walnut shells could be an alternative to the more expensive adsorbents used to remove the dye.

Keywords: Adsorption isotherm, Equilibrium, Kinetics, Methylene blue, Walnut shell.

1. Introduction

In recent years, industrial development has left its mark on society because many industries such as textiles, petrochemical, pesticide, paint, printing, metallurgical and pharmaceutical industries, among others, release large amounts of chemical compounds (such as colorants and pigments) generating pollution and environmental deterioration, [1] which has caused serious damage to the environment and health.

The textile industry produces wastewater that contains organic compounds with intense color, where in the dyeing processes, the percentage of dye lost in the wastewater is 50% in the fiber fixation levels and it is estimated that a substantial amount is discharged into wastewater annually [2].

The number of colorants they use, as well as heavy metals and dangerous substances, is so large that it has not been possible to calculate the total amount of these that are released uncontrolled into water bodies [3]. These compounds have aromatic structures that make them very stable and difficult to biodegrade [4]. Dyes can also be classified

according to their chromophore group into azo, anthraquinone, triphenylmethane, or imine dyes. Azoic and triphenylmethanes represent the majority of textile dyes [5,6] due to their properties of resistance to fixation and economic costs in the dyeing process. The release of pigmented waters into an ecosystem is a source of aesthetic pollution, which also causes disturbances in aquatic life. These pollutants are mutagenic, carcinogenic and cause severe damage to humans, such as dysfunction of the kidneys, reproductive system, liver, brain, and central nervous system in addition to allergies, skin irritation, nausea, sweating, vomiting, headache among other diseases [7]. MB is a dye that has a positive charge and is important for the textile industry, to dye leather materials and synthetic fibers. In the pharmaceutical area, it is used therapeutically to treat methemoglobinemia, psychiatric disorders, nervous system disorders and malaria [8-10]. Despite its many applications, it has been reported that acute exposure to MB can cause deleterious effects, such as cyanosis, vomiting, jaundice, tissue necrosis, tetraplegia, and increased heart rate in humans [11-12]. The MB average lethal oral dose (LD_{50}) in rats has been reported at 1,180 *mg/kg*. When low doses (10 *mg/kg*) were administered to rats, their blood pressure increased, while at high doses (20 *mg/kg*) systemic hypotension and hypertension worsened after endotoxemia [13, 14]. Although several studies have reported lethal doses in animals, limited data is available regarding this information in humans. However, it is hypothesized that the lethal dose is influenced by the dye′s effect on blood pressure, vascular resistance, and blood flow.

The textile industry is one of the many industries that discharge MB without any control, without any prior treatment, therefore these amounts exceed the permitted limit, which results in harmful effects on health and the environment. Furthermore, pigments impart toxicity in water bodies, including at low concentrations (less than 1 *mg/L*) [15] as they affect photosynthesis in aquatic organisms and plants due to the reduction of sunlight transmission [16].

Conventional methods for dye removal include coagulation, chemical oxidation, adsorption, ozonation, ion exchange, and flocculation, among others. Despite their benefits, some of them have relevant limitations [17-20] such as being usually effective and suitable only for small volumes of effluents and the need to treat very large amounts of by-products, which generates high costs.

In recent years, the use of low-cost and efficient alternative adsorbent materials in the removal of dyes from wastewater has been investigated. Some of these include palm and chitosan ash [20,21], grapefruit peel (*Citrus grandis*) [22], wheat peel [23,24]. WS as an agricultural residue could be an alternative to the wastewater treatment process. Due to the large amounts of this waste generated, it could be used to eliminate massive amounts of dyes from the textile industry, which causes a serious problem for the environment and the community.

In this work we propose the application of an agricultural residue as a low-cost adsorbent to remove MB from aqueous solutions. The main objective of this study was to evaluate the potential of WS as a low-cost adsorbent material in the removal of MB dye, widely used in the textile industry. Experimental parameters such as WS pH, WS dose, contact time, temperature and agitation have been investigated. Adsorption isotherms as well as adsorption kinetic curves were obtained and theoretical models were used to determine the adsorption mechanism. The results will be useful to know the feasibility of cheap

agricultural residues in the disposal of wastewater contaminated with pigments from the textile industry.

2. Materials and methods

2.1 Dye cationic

A cationic dye was used, MB (HYCEL, Monterrey, Mexico) with molecular formula $C_{16}H_{18}N_3ClS$ (319.85 *g/mol*), a wavelength of 650 *nm*, and its chromophore group is imine. The experiments were obtained from a 1000 *mg/L* stock solution that was prepared from the dye.

2.2 Pretreatment and characterization of WS

The WS, *Juglans regia* is a member of the family *Juglandaceae* was collected from Coahuila, Mexico. It was transferred in bags and washed with distilled water to remove impurities and soluble compounds that could interfere later in the tests. Before characterization and adsorption studies, the material was dried in an oven at a temperature of 60 °*C* for its subsequent grinding which was carried out in an industrial-type blender (USA Standard Test sieve). The adsorbent material was cut into small pieces and sieved until a particle size of 2 *mm* was obtained, which was stored in hermetic containers and did not receive any chemical treatment for the subsequent tests.

2.3 Characterization of WS

The characterization of the agricultural adsorbent material was analyzed by zeta point charge (ZPC) and isoelectric point (IEP) using a potentiometer, (Orion star A214 Potentiometer). Fourier transform infrared (FTIR) (Nicolet iS10 Thermo Spectrometer) was used for the identification of functional groups. WS surface morphology was also determined by scanning electron microscopy (SEM) analysis.

2.4 Experimental conditions for adsorption

For the adsorption tests, the following parameters were established as independent input variables, the adsorbent dose, temperature, agitation, and contact time, while the dye removal efficiency was chosen as the dependent response variable. A full factorial experimental design of 2^3 was designed, with three repetitions, resulting in a total of 24 experiments. The adsorption experiments were carried out in triplicate in 50 *ml* Erlenmeyer flasks where 0.1 *g* and 0.5 *g* of the adsorbent material were added with an initial 50 mg/L dye solution. Agitation was established at 50 and 100 *rpm* (Shaker MAXQ 4000 Thermo Scientific) at two temperatures, 293 and 313 *K* for 2 *h*, at neutral pH. After this time, the supernatant was separated and analyzed by a UV-visible spectrophotometer at 650 *nm* (EVOLUTION 60S ThermoScientific) to determine the removal capacity and final concentration of MB. The calculation of the dye removal percentage was evaluated according to the following equation:

$$\% R = \frac{C_o - C_e}{C_o} x\ 100 \qquad \textbf{(Eq. 1)}$$

Where:
C_o: Initial concentration (*mg/L*)
C_e: Concentration at equilibrium (*mg/L*)
The adsorption capacity, which is defined as the mass of adsorbate per gram of adsorbent, was evaluated using the equation:

$$q_m = \frac{(C_o - C_e)V}{W} \qquad \textbf{(Eq. 2)}$$

Where the C_o and C_t (*mg/L*) are the concentrations of the MB in the liquid phase at the beginning and equilibrium. *V* is the volume of the solution (*L*) and *W* is the mass of the dry adsorbent (*g*).

2.5 Batch kinetic studies

The adsorption tests for the kinetic study were carried out at different contact times of the adsorbent with the MB in a Thermo Scientific Shaker MAXQ 4000 at 293 *K*. The adsorption was carried out with 10 *mL* of MB with a concentration of 50 *mg/L* and 0.1*g* of WS with constant stirring at 50 *rpm* and 293 *K*. The experiment was carried out in triplicate at different times, 0, 5, 15, 30, 45, 60, 90 and 120 *min*. After each time, a sample was taken and centrifuged at 5000 *rpm* for 5 *min* to obtain the supernatant, which was analyzed by visible spectroscopy to obtain the final concentration of the dye and the percentage of removal.

The data obtained from the biosorption kinetics were analyzed using mathematical models of biosorption such as pseudo-first order and pseudo-second order, which explain the interactions of the dye molecules with the functional groups of the biosorbent cell wall.

2.6 Isotherm studies

Solutions with different concentrations of the dye were prepared from a stock solution of 500 *mg/L*. A 0.1*g* mass of the material biosorbent was added in 50 *mL* flasks containing the 10 *mL* solution of the dye at these concentrations (25, 50, 75, 100, 125, 150, 175, 200, 225, 250, 275, 300 *mg/L*). The dose and agitation that were established for this experiment were those that showed the highest removal percentages in the preliminary tests. Subsequently, the tubes were centrifuged at 5000 *rpm* for 5 *min*, the supernatant was separated and the residual concentration of the dye was measured by visible spectroscopy. The experiment was carried out in triplicate at 3 different temperatures (293 *K*, 303, and 313 *K*) for a time of 2 *h*. The experimental data obtained were used to analyze the Langmuir and Freundlich isotherms. After obtaining the experimental data, the adsorption isotherms were analyzed, among which the Langmuir and Freundlich models stand out, which describe how the adsorption of the liquid phase to the solid phase occurs on the surface of the biosorbent material.

3 Results and discussion

3.1 Characterization of WS as a function of surface pH, FTIR, and SEM.

The point of zero charge is an indicator of the number of positive and negative surface sites of the adsorbent material. Fig. 1a shows the pH value 5.0. This value indicates the most suitable range to achieve the elimination of a specific dye according to its anionic or cationic nature. Below this value, negatively charged dyes are absorbed, while above this value removal will be favored by positively charged dyes. On the other hand, this data also indicates that, below this value, the net charge of the adsorbent surface is positive, therefore, dyes that have a negative charge are absorbed, which is attributed to the presence of groups functional such as amino groups, which are positively charged and can attract negatively charged dyes such as anionic dyes. Whereas, above this value, the elimination of positively charged colorants can be favored.

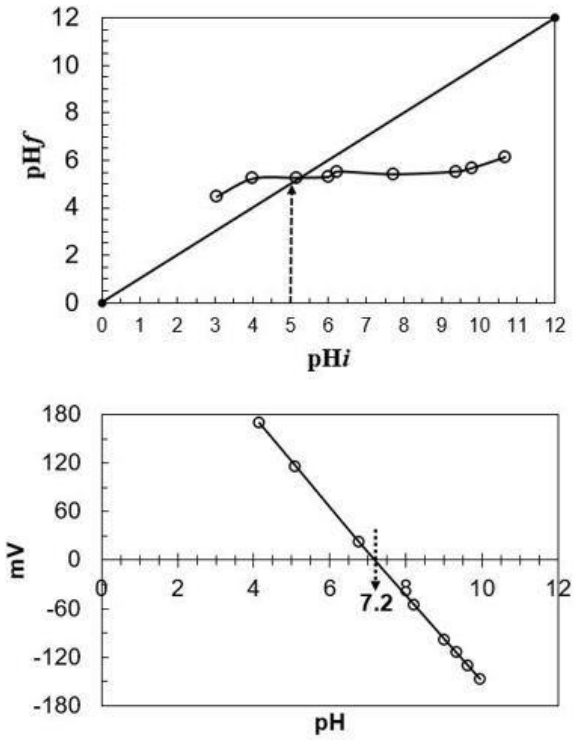

Figure 1. (a) Zero charge point (ZCP) **(b)** Isoelectric point (IEP) of WS.

The effect of pH in the aqueous solution is an important factor in the amount of adsorption. For example, [25] used the WS as an adsorbent for the removal of MB but treating the WS with different acids, such as hydrochloric acid, acid sulfuric, and phosphoric acid. Treatment with acids causes the adsorbent surface to undergo protonation or deprotonation of acidic and basic groups, also influencing the groups present in the MB molecule. They observed low adsorption of MB at low pH when the WS is not treated with acids, which can be attributed to the presence of hydrogen ions H^+ in the solution and the interaction with the cationic dye. This can lead to a decrease in the repulsion and adsorption charges of the adsorbate with the adsorbent. On the other hand, as the pH of the solution increases, the number of negative ions on the surface of the adsorbent increases, therefore high adsorption values would be expected, due to the strong electrostatic interaction between the negatively charged surface and MB which is a cationic dye.

However, Fig. 1b shows the isoelectric point with a value of 7.2, which indicates the surface charge distribution of the adsorbent material [26]. This value was decisive to know if WS would need any previous treatment for the experiments. Other studies such as [27] determined zero charge point using sunflower oil and activated carbon as adsorbent, obtaining values in a range of 2.5-5.5 [28], used coconut bagasse as adsorbent material for the removal of Blue Remazol (R160) which was 6.7. In other words, the adsorbent material was not chemically modified since the value obtained of 7.2 allowed the experiment to be carried out without altering the surface charge and the behavior of the WS with a cationic dye could be observed. The potentiometric titration of the biomass allowed us to determine the isoelectric point of the adsorbent surface which indicates that the WS can be used directly to see the behavior of dye of cationic nature such as MB, since these determinations also indicate the number of functional groups present on the surface, such as carboxyl and amino groups [29,30].

In the FT-IR analysis for WS, the different lengths related to the stretching vibrations can be observed, such as the one shown at 3301 cm^{-1}. Figure 2a and 2b this band it is related to the stretching vibration of the hydroxyl group present in the cellulose of agricultural residues. The band is shown at 2935 cm^{-1} was assigned to the stretch vibration of the aliphatic C–H group. The absorption band that appears at 1600 cm^{-1} is related to the C=O group that indicates the presence of carboxylic acids, ketones, or esters attributed to the precursor compounds of lignin [31-33]. The band show at 1520 cm^{-1} was assigned to the stretching vibration of C=C groups, while the 1436 cm^{-1} band suggests bending

vibrations of methyl and methylene groups. On the other hand, the agricultural adsorbent materials are attributed infrared spectra with basic components that correspond to the bands of carboxylic acid (1714 and 1032 cm^{-1}), carboxylate ion (1348 and 1606 cm^{-1}), and the presence of the amino group (1243 and 1032 cm^{-1}). The presence of these groups is an indication of the importance of functional groups on the surface of WS since these ionizable groups preferentially favor the elimination of cationic dyes.

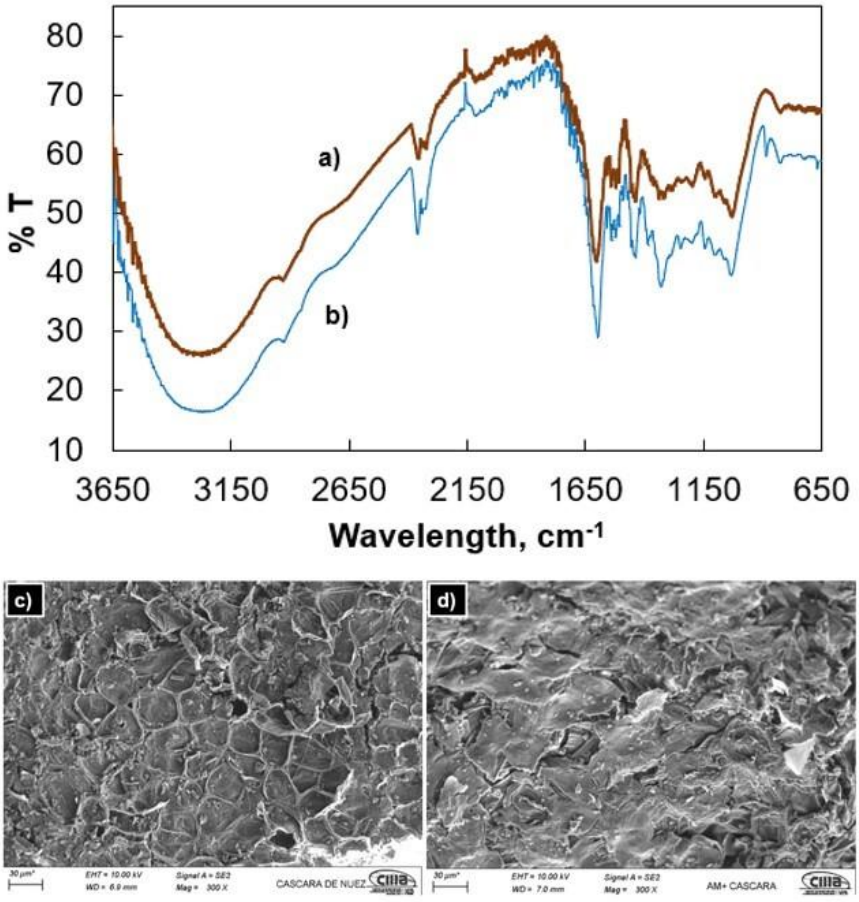

Figure 2. FT-IR of WS adsorbent; (a) before dye adsorption (b) after dye adsorption. SEM characterization; (c) before MB adsorption (d) after MB adsorption.

Scanning microscopy analysis shows the micrographs for the WS and MB treatment. Fig. 2c shows the surface for the WS without receiving prior treatment, the measurement was made at 30 μm in which a surface with pores of irregular size can be seen, a hollow surface with high porosity, these irregularities allow the adsorption of dyes on the surface of the WS, due to the presence of holes, pores, and cracks. Fig. 2d shows the WS surface after adsorption with MB, it can be seen that the holes and pores have been occupied by the MB molecules, the MB molecules covered the WS surface, they show some superficial scars, but in general, they tend to occupy the holes homogeneously. This analysis confirms that the adsorption of MB on the WS has been successful. In general, the morphologies of agricultural residues have been studied and these characteristics that are observed are particular to lignocellulosic materials, which

generally present unlimited pores and irregular porous structures.

3.2 Experimental conditions for adsorption

The parameters that were considered to evaluate the experimental conditions of the adsorption process were the following: adsorbent dose (*g*), temperature (*K*) and agitation (*rpm*), all of these as a function of time. Final concentration, removal capacity and removal efficiency were evaluated as dependent response variables. In fig. 3 the experimental adsorption conditions for MB are shown. It started with a concentration of 50 *mg/L* with a reaction time of 2 *h*. The removal percentages at 293 *K* were 95 ± 5.2% while at 313 *K* they were 95 ± 4.7%. The initial concentration of the dye was not a variable to modify, however, it is an important factor to consider the mass transfer process between the adsorbent and the adsorbate.

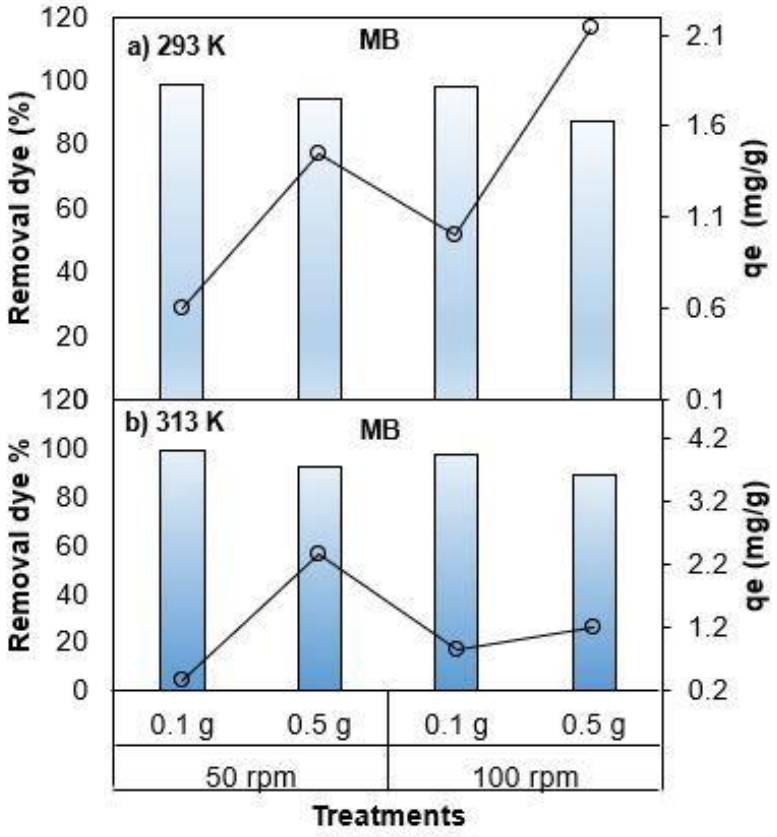

Figure 3. Experimental optimization conditions of MB (**a)** At a temperature 293 *K* (**b)** At a temperature 313 *K*. The left y-axis represents the percentage of dye removal (bars) and the right represents the removal capacity (line). The x-axis shows the adsorbent and agitation doses.

It has been shown that the percentage of dye removal decreases when the initial concentration is high (*150 mg/L*) [34], due to the saturation of the active adsorption sites on the surface of the adsorbent, while with low initial concentrations the adsorption sites were unoccupied, so the adsorption sites can be easily occupied by the dye without becoming saturated, thus achieving an increase in the percentage of dye removal. Studies have shown an increase in the removal rate of MB at different changes in initial dye concentration. Jawad et al. (2018) used dragon fruit peels in MB removal but

without further treatment [35]. The removal efficiency reached its optimal performance around 83%, at a dose of adsorbent of 600 *mg/L*, temperature 298 *K*, initial dye concentration 100 *mg/L*, stirring speed of 120 *rpm*, and contact time of 180 *min*. Shen and Gondal (2017) [36] used coffee powder, from an initial concentration of 15 *mg/L* of colorant, pH 2 and dose of adsorbent 0.05 g/L for the removal of Rhodamine B and Rhodamine 6G.

3.2.1 Statistical analysis

The experimental design was carried out using the Minitab 19 tool, applying the removal percentage of removal or adsorption efficiency as response variables. ANOVA factorial design 2^3 ($p < 0.05$) was used with a total of 24 experiments, the variables of temperature, adsorbent dose, and agitation. Each variable was assigned by letters, (A) for temperature, (B) for the adsorbent dose, and (C) for agitation. Two levels were handled, high level (+) and low level (-), 3 replicates were made and the response factor was the removal percentage.

In Table 1, it can be deduced that for MB the factors B and C are quite significant in the analyzed response, as well as the BC interaction. On the other hand, factor A does not add significant value to the response, so it is convenient to manage it at the level that represents the lowest energy consumption and represents the lowest cost, that is, at 20 °C.

Table 1. Two-level factors for ANOVA analysis. Statistical parameters of the data obtained in the ANOVA analysis.

Assigned letter	**Factor**		**Low level (-)**		**High level (+)**	
A	Temperature (K)		293		313	
B	Dose (g)		1		5	
C	Agitation (rpm)		50		100	
Source	**DF**	**S.S.S**	**Contribution**	**SS fit**	**LS**	**F value**
Model	3	366.21	82.34%	366.21	122.069	31.08
Linear	2	328.71	73.91%	328.71	164.353	41.85
B	1	291.21	65.48%	291.21	291.207	74.15
C	1	37.50	8.43%	37.50	37.500	9.55
2 term interactions	1	37.50	8.43%	37.50	37.500	9.55
B*C	1	37.50	8.43%	37.50	37.500	9.55
Error	20	78.55	17.66%	78.55	3.927	
Lack of fit	4	15.58	3.50%	15.58	3.895	0.99

The model shown suggests that, using factor B at the low level (1*g* dose) and factor C at the high level (stirring 100 *rpm*), 98 *%* removal is obtained. The ANOVA in Table 1b also shows the BC interaction and it is strongly significant, so it is suggested that, when factor B is at a low level (-), factor C can be used at a low level (-) or at a high level. (+) since it generates the same response, therefore we could handle factor C with the low level.

3.3 Effect of adsorbent dose

One of the main factors that affect the adsorption process is the dose of the adsorbent material, this is due to the fact that the surface of this material has adherence or adsorption sites and this number of sites increases when working with high doses. since the promoted surface is more exposed to the adsorbate and its molecules find a place to settle or rest during the adsorption process. However, when the dose of the adsorbent is very high, saturation of these adsorption sites

can occur, which can result in a decrease in the efficiency of dye removal [37].

In figure 3 we can see the effect of the adsorbent dose on the removal percentage at two fixed temperatures and with an initial MB concentration of 50 *mg/L*. In general, it is known that the increase in the number of adsorption sites on the surface of the adsorbent leads to an increase in the removal efficiency [38], for MB the removal percentages remained above 88%, the effect of the dose reflected high percentages of removal even when the dose was low, this effect was pointed out in the statistical analysis, it was even suggested that it is possible to work at a minimum dose since both doses are effective on the removal of dyes. Therefore, the choice of the minimum dose can also be an important factor of economic interest for the agro-industrial sector. The data obtained led to the decision that the optimal experimental dose to continue with the other study experiments is 0.1 *g* of WS.

The effect of the dose was also studied with other dyes such as indigo carmine but with rice husk as adsorbent material, from this study it was concluded that the removal efficiency was 36 – 96 % when the doses of the adsorbent were varied from 2 at 20 *g/L* [39]. Similar results were obtained by Fatma Bouaziza et al., 2017 when they used almond gum as an adsorbent for the adsorption of malachite green. The study was carried out by varying the dose of the adsorbent from 2 to 30 *g/L*, starting from an initial concentration of 100 *mg/L* at 40 °*C* and neutral pH for a contact time of 1 h [40]. On the other hand, Mohammad Kashif Uddin and Abu Nasar, 2020 [41] observed an increase in the percentage of MB removal when they varied the dose of WS (*Junglans regia*) from 0.1 to 1 *g*, their results were very similar to those of this work, since they obtain percentages of removal above 90 % at low doses, this may be due to the increased interactions of the molecule with the adsorbate at low doses and the provision of active sites, which at higher doses where a supersaturation of the adsorbate with the adsorbent can occur, causing a decrease in dye removal.

3.4 *Effect of temperature*

The temperature factor is another important parameter during the adsorption process. This is an indicator of the nature of the adsorption, since it is known that an increase in temperature causes an increase in the mobility of the active sites of the adsorbent, thus causing an increase in the rate of diffusion of the molecules in the interface, that is, in the boundary layer that divides the dye molecules and the internal pores of the adsorbate particles [42]. This effect can also vary depending on the movement of the dye molecules and the class to which they belong. With the temperature variation, a variation in the equilibrium capacity of the adsorbent is also expected. If the adsorption capacity increases with increasing temperature, an endothermic process is said to take place [43], this increase in temperature causes an increase in the number of sites of the adsorbent material. Figures 3a and 3b show the temperature variation of 293 *K* and 313 *K* for MB, in which it can be seen that as the temperature increases, the elimination percentages remain above 90%. The increase in adsorption capacity may also be due to the effect of junction fractures on the surface of the adsorbent. [44], It is worth mentioning that the adsorption process can become slow when working with temperatures higher than 313 *K*, since the adsorption sites of the adsorbent material could become saturated, and probably the adsorbate molecules in the adsorbent would initiate a desorption process if the process continues with [45,46] high temperatures. The adsorption of MB with palm kernel fiber as adsorbent material was

also studied, which was treated with HCl, when the temperature increased from 299-339 *K*, an increase in the adsorption capacity was observed, which indicates that the adsorption process is carried endothermically [47], similar studies were carried out by [48], when they studied the adsorption of MB, malachite green (MG) and crystal violet (CV).

3.5 Adsorption kinetic studies

To define the adsorption efficiency, it is necessary to describe the adsorption dynamics in terms of adsorption kinetics by measuring the adsorption residence times and the rate constant [49]. It is suggested that for a material to be useful as an adsorbent, it must have a good adsorption rate, that is, it must have a high adsorption capacity and therefore a fast adsorption rate. This adsorption process involves primarily the internal mass transfer of the adsorbate molecules to the sorption sites, as well as the external mass transfer of the dye molecules from most of the solution to the external surface of the adsorbent and therefore last the sorption process itself.

The pollutant biosorption process is dependent on the time required to reach equilibrium and this can be measured by biosorption kinetics experiments. In many dye adsorption processes, the pseudo-first-order and pseudo-second-order models are used to determine adsorption kinetics. The pseudo-first-order model is given by the Lagergren expression [50], to determine the adsorption rate constant. It is worth mentioning that there is evidence of dye removal registers in which the pseudo-first-order model does not fit well to the entire contact time range, however, it is one of the oldest and most theoretical models that can predict the amount of dye adsorbed onto the adsorbent material.

$$\ln(q_e - q_t) = \ln q_e - k_1 t \qquad \textbf{(Eq. 3)}$$

Where q_e and q_t *(mg/g)* represent the number of dyes adsorbed at equilibrium and at time *t(min)*, respectively, and k_1 *(l/min)* is the adsorption constant. Table 2 showed the adsorption kinetic data for the MB starting from an initial concentration of 50 *mg/l*. The pseudo-first-order and Elovich models showed low correlation coefficients compared to the pseudo-second-order. The expression of the pseudo-second-order model is given by [51].

$$\frac{t}{q_t} = \frac{1}{k_2 q_e^2} + \frac{1}{q_e} \qquad \textbf{(Eq. 4)}$$

Where q_e represents the adsorption capacity at equilibrium and k_2 is the pseudo-second-order constant *(g/mg·min*) which can be experimentally determined from the slope and intersection of the line by graphing *t/q (min·g/mg) vs t(min)*. The results of the kinetic models are shown in Table 2.

Table 2. Parameters of kinetic models for MB dye at 313 *K* and initial concentration of 50 *mg/L*.

Kinetic model	Parameters	
pseudo first order	k, (*l/min*) q_e, (*mg/g*) R^2	0.586 0.0001 **0.029**
pseudo second order	k, (*g/mg min*) q_e, (*mg/g*) R^2	2.820 4.027 **0.9974**
Ecuación de Elovich	A, (*mg/g min*) b, (*g/mg*) R^2	0.019 30.674 **0.749**

The pseudo-first order model shows very inaccurate R^2 values, deviated from unity, and the value of q_e turned out to be too small. In contrast, the graph of *t/q vs. t* (Figure 4) for the pseudo-second order model showed R^2 values of 0.9974 for MB, this value is close to unity and an increase in the value could also be seen. of what. Therefore, based on the R^2 values and the fit of the theoretical *qe* and *t/qe* value with the experimental one, we can assume that the MB adsorption fits the pseudo-second order model well. The pseudo-second order model assumes that the mass transfer is explained by the chemisorption mechanism, due to the participation of chemical forces involved in the chemical bonding of the MB with the WS surface and that it may also be the control stage of the speed in adsorption processes by [52,53]. The pseudo-second order model assumes that chemisorption is strongly involved in controlling the rate of adsorption processes. Figure 4 represents the fitted model for MB, which shows a correlation coefficient close to unity and fits a pseudo second order model. This pattern was also observed in MB adsorption with peanut shells [54].

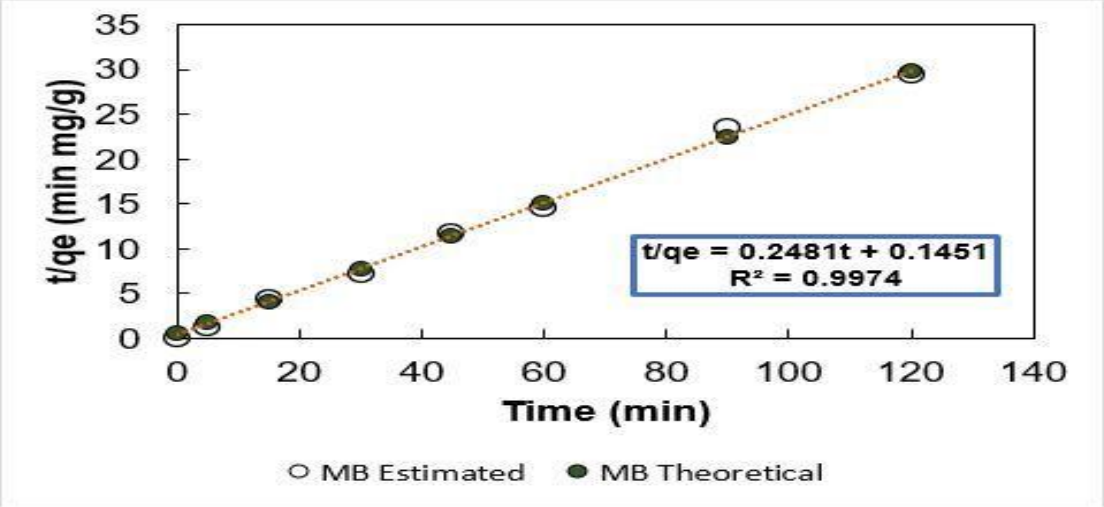

Figure 4. Pseudo-second order kinetics for adsorption of MB on WS waste in an aqueous solution of 50 mg/L at 313 *K*.

On the other hand, [55,56] also studied MB adsorption using guava leaf powder in which they obtained R^2 values for the pseudo first order model with values ranging between 0.70 and 0.85, while the R^2 values of the pseudo second order model were 0.99. The Elovich equation has also been widely used to describe the process of adsorption of contaminants from water, such as heavy metal effluents such as Cr(VI) and Cu(II) when chitin and chitosan were used as adsorbent materials. This model is of general application in chemisorption processes and assumes that the active sites of the adsorbent are heterogeneous [57] and therefore exhibit different activation energies, which confirms the second order reaction for a heterogeneous reaction process.

3.6 Isotherms adsorption

Contaminants migrating from an aqueous phase to an agricultural adsorbent have been studied by many isothermal models [58, 59]. The ratio of the adsorbate in the liquid phase and the equilibrium adsorption amount on the solid phase at a given temperature can be determined from the adsorption isotherms. To establish the adsorption data, as well as the

adsorption mechanisms and the maximum adsorption capacity, two isotherm models were tested: Langmuir and Freundlich. These models allow us to model the equilibrium data, study the adsorption mechanism, the maximum adsorption capacity, as well as the properties of the adsorbent material.

The Langmuir isotherm accounts for surface coverage by balancing relative adsorption and desorption rates (dynamic equilibrium). Adsorption is proportional to the fraction of the adsorbent surface that is open while desorption is proportional to the fraction of the adsorbent surface that is covered [60]. It is worth mentioning that one of the tools applied to define the best model to quantify the adsorbate distribution is through linear regression analysis [61]. The Langmuir adsorption model establishes the maximum adsorption, which suggests that, once the adsorbate is adsorbed, it does so occupying a single site, that is, adsorption occurs in specific homogeneous sites, to form a monolayer of molecules on the surface of the adsorbent. Furthermore, this model assumes that there is no steric hindrance between the adsorbed molecules. The Langmuir equation in linear form is [62]:

$$\frac{C_e}{q_e} = \frac{1}{q_{max} * K} + \frac{C_e}{q_{max}} \qquad \textbf{(Eq. 4)}$$

Where C_e *(mg/L)* is the equilibrium concentration of the adsorbate, q_e *(mg/g)* is the amount of adsorbate per unit mass of adsorbent, K and q_{max} are Langmuir constants related to adsorption capacity and rate of adsorption, respectively.

The Freundlich model is oriented to adsorption processes that occur on heterogeneous surfaces [63]. This model defines the heterogeneity of the surface and the exponential distribution of the active sites and their energies [64]. The equation of the Freundlich model in linear form is the following [65]:

$$\log q_e = \log K_F + \frac{1}{n} \log C_e$$

Where K_F is the adsorption capacity (*L/mg*) and $1/n$ is the adsorption intensity; this is also an indicator of the relative distribution of the energy and heterogeneity of adsorbate sites.

The applicability of the isotherm equations was compared by judging the correlation coefficients, R^2. Table 3 shows that the Langmuir isotherm model produced R^2 values close to unity as the temperature increases. The R^2 values (0.88) suggest that the Langmuir isotherm provides a good fit to the isotherm data, although the higher temperature Freundlich model also shows R^2 values very similar to the Langmuir ones, this could be seen as a competition of adsorption mechanisms, this indicates that the MB could carry out the two adsorption models with increasing temperature.

Table 3. Parameters of isothermal adsorption models for MB dye.

Isotherm Model	***Parameters***	***Temperature (K)***		
		293	**303**	**313**
Langmuir	q_e (*mg/g*)	80.65	42.92	62.11
	b (*L/mg*)	0.01	0.02	0.02
	K	8.48	31.41	44.04
	R^2	**0.78**	**0.32**	**0.88**
Freundlich	*n*	2.02	1.27	3.55
	K_F *(L/mg)*	0.37	0.52	0.17
	R^2	**0.72**	**0.68**	**0.84**

The MB describes two models that compete for the accommodation of the molecules, firstly, it fits the monolayer model but the multilayer phenomenon can also occur if the temperature continues to increase, which means that the interaction between the adsorbent and adsorbate occurs first by chemisorption, but as the temperature increases, physisorption may occur.

A similar observation was reported for MB adsorption on silkworms [66], cedar sawdust, and crushed brick [67]. Table 4 lists the comparison between the MB monolayer adsorption capacities on various adsorbents. It is clear that the WS used in this work had a relatively adequate adsorption capacity of 80.65 mg/g compared to other adsorbents found in the literature [68-71].

Table 4. Comparison of the maximum monolayer adsorption of MB onto various adsorbents.

Adsorbents	Maximum monolayer adsorption capacity (mg/g)	References
Walnut shell	80.65	This work
Sawdust	40.50	[68]
Oil palm trunk fiber	49.35	[69]
Broad dean peels	62.72	[70]
Jute processing waste	22.47	[71]

3.6.1 Thermodynamic studies

There are thermodynamic parameters that are of importance in the adsorption process since these allow us to predict whether the mechanism of the adsorption process occurs by physisorption or chemisorption [72,73]. These parameters include enthalpy ($\Delta H°$), entropy ($\Delta S°$), and Gibbs free energy ($\Delta G°$), which are determined by the following equations and from the Van't Hoff intersection and slope.

$$\Delta G° = -RT \ln K_c$$

$$\ln K_c = \frac{-\Delta H°}{RT} + \frac{\Delta S°}{R}$$

Where:

R is the universal gas constant (8.314 *J /mol/K*), K_c is the dimensionless equilibrium constant derived from the dimensional distribution coefficient K_d with the dimension of *L/g*. K_d at different temperatures is obtained by plotting q_e / C_e *vs* C_e and extrapolating C_e to zero.

The results with negative values of $\Delta G°$ indicate that the adsorption process is spontaneous and favorable in this temperature range. It can be observed in the table 5, that for MB the $\Delta G°$ values do not show a tendency to increase or decrease with increasing temperature, which is confirmed by the statistical analysis of ANOVA, which showed that temperature does not significantly affect efficiency removal.

Table 5. Thermodynamic parameters for the adsorption of MB with WS.

Temperature (K)	ΔG° (kJ/mol)	ΔH° (kJ/mol)	ΔS° (kJ/mol)
293	-21157.32	1097.02	-2.63
303	-23363.13		
313	-17333.87		

Positive values of $\Delta H°$ indicate an adsorption process of an endothermic nature. The $\Delta S°$ is an indicator of the disorder of the molecules at the adsorbent and adsorbate interface. Negative values of $\Delta S°$ suggest that the disorder of the MB molecules decreases, which means that these colored molecules are deposited on the WS surface without modifying the internal structure of the adsorbent during the entire adsorption process. On the contrary, positive values of $\Delta S°$ indicate that the disorder increases so that the molecules can adhere or unattached to the surface of the adsorbent, that is to say, that some of these particles can bind to the WS but for a short time and then disjoin.

4 Conclusions

Current studies showed that the adsorption of MB with WS is favored by low agitation, low temperature, and low adsorbent doses. The adsorption kinetics followed a pseudo-second-order kinetic model. The results obtained were modeled using two isotherm models: Langmuir and Freundlich. The equilibrium isotherms were well described by the Langmuir equation, giving a maximum adsorption capacity of 80.65 *mg/g* at 293 *K*. The thermodynamic parameters suggest that adsorption is a typical characteristic of chemisorption, in a spontaneous process and endothermic. This study revealed that WS can be used as an inexpensive method. Natural-based adsorbent to remove MB stains from aqueous solutions. When the WS used as an adsorbent becomes saturated, it can be incinerated. Since WS production occurs in the middle of the year in most tropical countries, the wasted shell can be easily purchased and used for future commercial applications.

5 Acknowledgment

We thank the National Council of Science and Technology (CONAHCyT-Mexico) for the support provided as Ph.D. scholarship. We also thank the PAICYT 2021 project which provided support for this research.

6 References

1. Jacob, J. M., Karthik, C., Saratale, R. G., Kumar, S. S., Prabakar, D., Kadirvelu, K., & Pugazhendhi, A. (2018). Biological approaches to tackle heavy metal pollution: a survey of literature. *Journal of environmental management*, *217*, 56-70. http://doi.org/10.1016/j.jenvman.2018.03.077

2. Zainith, S. U. R. A. B. H. I., Sandhya, S., Saxena, G. A. U. R. A. V., & Bharagava, R. N. (2016). Microbes: Ecofriendly tools for the treatment of industrial wastewater. *Microbes and Environmental Management*, *2016*, 75-100.

3. Mani, S., Chowdhary, P., & Bharagava, R. N. (2019). Textile wastewater dyes: Toxicity profile and treatment approaches. *Emerging and Eco-friendly Approaches for Waste Management*, 219-244. http://doi.org/10.1007/978-981-10-8669-4_11

4. Aksu, Z. (2005). Application of biosorption for the removal of organic pollutants: A review. *Process Biochemistry*, *40*(3-4), 997-1026. http://doi.org/10.1016/j.procbio.2004.04.008

5. Yang, X. Q., Zhao, X. X., Liu, C. Y., Zheng, Y., & Qian, S. J. (2009). Decolorization of azo, triphenylmethane and anthraquinone dyes by a newly isolated *Trametes sp*. SQ01 and its laccase. *Process Biochemistry*, *44*(10), 1185-1189.

http://doi.org/10.1016/j.procbio.2009.06.015

6. Forgacs, E., Cserháti, T., & Oros, G. (2004). Removal of synthetic dyes from wastewaters: A review. *Environment International*, *30*(7), 953-971. http://doi.org/10.1016/j.envint.2004.02.001

7. Al-Ghouti, M. A., & Sweleh, A. O. (2019). Optimizing textile dye removal by activated carbon prepared from olive stones. *Environmental Technology & Innovation*, *16*, 100488. http://doi.org/10.1016/j.eti.2019.100488

8. Oz, M., Lorke, D. E., Hasan, M., & Petroianu, G. A. (2011). Cellular and molecular actions of methylene blue in the nervous system. *Medicinal Research Reviews*, *31*(1), 93-117. http://doi.org/10.1002/med.20177

9. Lu, G., Nagbanshi, M., Goldau, N., Mendes Jorge, M., Meissner, P., Jahn, A., ... & Mueller, O. (2018). Efficacy and safety of methylene blue in the treatment of malaria: A systematic review. *BMC Medicine*, *16*, 1-16. http://doi.org/10.1186/s12916-018-1045-3

10. Bosoy, D., Axelband, J., Pursell, R. N., Lukaszczyk, J. J., & Stawicki, S. P. (2017). Utilization of methylene blue in the setting of hypotension associated with concurrent renal and hepatic failure: A concise review. *International Journal of Academic Medicine*, *3*(Suppl 1), S101-S111. http://doi.org/10.4103/IJAM.IJAM_88_16

11. Kumar, K. V., Ramamurthi, V., & Sivanesan, S. (2005). Modeling the mechanism involved during the sorption of methylene blue onto fly ash. *Journal of Colloid and Interface Science*, *284*(1), 14-21. http://doi.org/10.1016/j.jcis.2004.09.063

12. Vadivelan, V., & Kumar, K. V. (2005). Equilibrium, kinetics, mechanism, and process design for the sorption of methylene blue onto rice husk. *Journal of Colloid and Interface Science*, *286*(1), 90-100. http://doi.org/10.1016/j.jcis.2005.01.007

13. Seif, C., Portillo, F. J. M., Osmonov, D. K., Böhler, G., van der Horst, C., Leissner, J., ... & Braun, P. M. (2004). Methylene blue staining for nerve-sparing operative procedures: An animal model. *Urology*, *63*(6), 1205-1208. http://doi.org/10.1016/j.urology.2003.12.020

14. Zhang, H., Rogiers, P., Preiser, J. C., Spapen, H., Manikis, P., Metz, G., & Vincent, J. L. (1995). Effects of methylene blue on oxygen availability and regional blood flow during endotoxic shock. *Critical Care Medicine*, *23*(10), 1711-1721. http://doi.org/10.1097/00003246-199510000-00016

15. Lian, L., Guo, L., & Guo, C. (2009). Adsorption of Congo red from aqueous solutions onto Ca-bentonite. *Journal of Hazardous Materials*, *161*(1), 126-131. http://doi.org/10.1016/j.jhazmat.2008.03.063

16. Malik, R., Ramteke, D. S., & Wate, S. R. (2007). Adsorption of malachite green on groundnut shell waste-based powdered activated carbon. *Waste Management*, *27*(9), 1129-1138. http://doi.org/10.1016/j.wasman.2006.06.009

17. Sulak, M. T., Demirbas, E., & Kobya, M. (2007). Removal of Astrazon Yellow 7GL from aqueous solutions by adsorption onto wheat bran. *Bioresource Technology*, *98*(13), 2590-2598. http://doi.org/10.1016/j.biortech.2006.09.010

18. Daneshvar, N., Ayazloo, M., Khataee, A. R., & Pourhassan, M. J. B. T. (2007). Biological decolorization of dye solution containing Malachite Green by microalgae *Cosmarium* sp. *Bioresource Technology*, *98*(6), 1176-1182. http://doi.org/10.1016/j.biortech.2006.05.025

19. Kumar, C. G., Mongolla, P., Joseph, J., & Sarma, V. U. M. (2012). Decolorization and biodegradation of triphenylmethane dye, brilliant green, by *Aspergillus* sp. isolated from Ladakh, India. *Process Biochemistry*, *47*(9), 1388-1394. http://doi.org/10.1016/j.procbio.2012.05.015

20. Ahmad, A. A., Hameed, B. H., & Aziz, N. (2007). Adsorption of direct dye on palm ash: Kinetic and equilibrium modeling. *Journal of Hazardous Materials*, *141*(1), 70-76. http://doi.org/10.1016/j.jhazmat.2006.06.094

21. Hasan, M., Ahmad, A. L., & Hameed, B. H. (2008). Adsorption of reactive dye onto cross-linked chitosan/oil palm ash composite beads. *Chemical Engineering Journal*, *136*(2-3), 164-172. http://doi.org/10.1016/j.cej.2007.03.038

22. Hameed, B. H., Mahmoud, D. K., & Ahmad, A. L. (2008). Sorption of basic dye from aqueous solution by pomelo (*Citrus grandis*) peel in a batch system. *Colloids and Surfaces A: Physicochemical and Engineering Aspects*, *316*(1-3), 78-84. http://doi.org/10.1016/j.colsurfa.2007.08.033

23. Gupta, V. K., Jain, R., Varshney, S., & Saini, V. K. (2007). Removal of Reactofix Navy Blue 2 GFN from aqueous solutions using adsorption techniques. *Journal of Colloid and Interface Science*, *307*(2), 326-332. http://doi.org/10.1016/j.jcis.2006.12.003

24. Gupta, V. K., Jain, R., & Varshney, S. (2007). Removal of Reactofix golden yellow 3 RFN from aqueous solution using wheat husk—an agricultural waste. *Journal of Hazardous Materials*, *142*(1-2), 443-448. http://doi.org/10.1016/j.jhazmat.2006.08.048

25. Coşkun, R., Yıldız, A., & Delibaş, A. (2017). Removal of methylene blue using fast sucking adsorbent. *Journal of Materials and Environmental Science*, *8*, 398-409.

26. Poghossian, A. A. (1997). Determination of the pHpzc of

insulators surface from capacitance–voltage characteristics of MIS and EIS structures. *Sensors and Actuators B: Chemical*, *44*(1-3), 551-553. http://doi.org/10.1016/S0925-4005(97)00156-1

27. Karagöz, S., Tay, T., Ucar, S., & Erdem, M. (2008). Activated carbons from waste biomass by sulfuric acid activation and their use on methylene blue adsorption. *Bioresource technology*, *99*(14), 6214-6222. http://doi.org/10.1016/j.biortech.2007.12.019

28. Vieira, A. P., Santana, S. A., Bezerra, C. W., Silva, H. A., Chaves, J. A., de Melo, J. C., ... & Airoldi, C. (2009). Kinetics and thermodynamics of textile dye adsorption from aqueous solutions using babassu coconut mesocarp. *Journal of Hazardous Materials*, *166*(2-3), 1272-1278. http://doi.org/10.1016/j.jhazmat.2008.12.043

29. Radovic, L. R., Silva, I. F., Ume, J. I., Menéndez, J. A., Leon, C. L. Y., & Scaroni, A. W. (1997). An experimental and theoretical study of the adsorption of aromatics possessing electron-withdrawing and electron-donating functional groups by chemically modified activated carbons. *Carbon*, *35*(9), 1339-1348. http://doi.org/10.1016/S0008-6223(97)00072-9

30. Savova, D., Petrov, N., Yardim, M. F., Ekinci, E., Budinova, T., Razvigorova, M., & Minkova, V. (2003). The influence of the texture and surface properties of carbon adsorbents obtained from biomass products on the adsorption of manganese ions from aqueous solution. *Carbon*, *41*(10), 1897-1903. http://doi.org/10.1016/S0008-6223(03)00179-9

31. Dahri, M. K., Kooh, M. R. R., & Lim, L. B. (2014). Water remediation using low cost adsorbent walnut shell for removal of malachite green: equilibrium, kinetics, thermodynamic and regeneration studies. *Journal of Environmental Chemical Engineering*, *2*(3), 1434-1444. http://doi.org/10/1016/j.jece.2014.07.008

32. Miyah, Y., Lahrichi, A., Idrissi, M., Khalil, A., & Zerrouq, F. (2018). Adsorption of methylene blue dye from aqueous solutions onto walnut shells powder: equilibrium and kinetic studies. *Surfaces and Interfaces*, *11*, 74-81. http://doi.org/10.1016/j.surfin.2018.03.006

33. Song, J., Zou, W., Bian, Y., Su, F., & Han, R. (2011). Adsorption characteristics of methylene blue by peanut husk in batch and column modes. *Desalination*, *265*(1-3), 119-125. http://doi.org/10.1016/j.desal.2010.07.041

34. Eren, Z., & Acar, F. N. (2006). Adsorption of Reactive Black 5 from an aqueous solution: equilibrium and kinetic studies. *Desalination*, *194*(1-3), 1-10. http://doi.org/10.1016/j.desal.2005.10.22

35. Jawad, A. H., Kadhum, A. M., & Ngoh, Y. S. (2018). Applicability of dragon fruit (Hylocereus polyrhizus) peels as low-cost biosorbent for adsorption of

methylene blue from aqueous solution: kinetics, equilibrium and thermodynamics studies. *Desalin Water Treatment*, *109*(2018), 231-240. http://doi.org/10.5004/dwt.2018.21976

36. Shen, K., & Gondal, M. A. (2017). Removal of hazardous Rhodamine dye from water by adsorption onto exhausted coffee ground. *Journal of Saudi Chemical Society*, *21*, S120-S127. http://doi.org/10.1016/j.jscs.20.13.11.005

37. Mittal, A., Mittal, J., Malviya, A., & Gupta, V. K. (2010). Removal and recovery of Chrysoidine Y from aqueous solutions by waste materials. *Journal of Colloid and Interface Science*, *344*(2), 497-507. http://doi.org/10.1016/j.jcis.2010.01.007

38. Ofomaja, A. E. (2008). Sorptive removal of Methylene blue from aqueous solution using palm kernel fibre: Effect of fibre dose. *Biochemical Engineering Journal*, *40*(1), 8-18. http://doi.org/10.1016/j.bej.2007.11.028

39. Lakshmi, U. R., Srivastava, V. C., Mall, I. D., & Lataye, D. H. (2009). Rice husk ash as an effective adsorbent: Evaluation of adsorptive characteristics for Indigo Carmine dye. *Journal of Environmental Management*, *90*(2), 710-720. http://doi.org/10.1016/j.jenvman.2008.01.002

40. Bouaziz, F., Koubaa, M., Kallel, F., Ghorbel, R. E., & Chaabouni, S. E. (2017). Adsorptive removal of malachite green from aqueous solutions by almond gum: kinetic study and equilibrium isotherms. *International Journal of Biological Macromolecules*, *105*, 56-65. http://doi.org/10.1016/j.ijbiomac.2017.06.106

41. Uddin, M. K., & Nasar, A. (2020). Walnut shell powder as a low-cost adsorbent for methylene blue dye: isotherm, kinetics, thermodynamic, desorption and response surface methodology examinations. *Scientific Reports*, *10*(1), 7983. http://doi.org/10.1038/s41598-020-64745-3

42. Uddin, M. K., & Nasar, A. (2020). Walnut shell powder as a low-cost adsorbent for methylene blue dye: isotherm, kinetics, thermodynamic, desorption and response surface methodology examinations. *Scientific Reports*, *10*(1), 7983. http://doi.org/10.1038/s41598-020-64745-3

43. Nandi, B. K., Goswami, A., & Purkait, M. K. (2009). Removal of cationic dyes from aqueous solutions by kaolin: kinetic and equilibrium studies. *Applied Clay Science*, *42*(3-4), 583-590. http://doi.org/10.1016/j.clay.2008.03.015

44. Gündüz, F., & Bayrak, B. (2017). Biosorption of malachite green from an aqueous solution using pomegranate peel: equilibrium modelling, kinetic and thermodynamic studies. *Journal of Molecular Liquids*, *243*, 790-798.

http://doi.org/10.1016/j.molliq.2017.08.095

45. Saeed, K., Ishaq, M., Sultan, S., & Ahmad, I. (2016). Removal of methyl violet 2-B from aqueous solutions using untreated and magnetite-impregnated almond shell as adsorbents. *Desalination and Water Treatment*, *57*(29), 13484-13493. http://doi.org/10.1080/19443994.2015.1058191

46. İmamoğlu, M. (2014). Adsorption of methylene blue from aqueous solutions by activated carbon prepared from hazelnut husk using zinc chloride. *Journal of Applied Analytical and Environmental Chemistry*. http://doi.org/10.1016/j.jaap.2014.09.006

47. Ofomaja, A. E. (2008). Sorptive removal of Methylene blue from aqueous solution using palm kernel fibre: Effect of fibre dose. *Biochemical Engineering Journal*, *40*(1), 8-18. http://doi.org/10.1016/j.bej.2007.11.028

48. Önal, Y. (2006). Kinetics of adsorption of dyes from aqueous solution using activated carbon prepared from waste apricot. *Journal of Hazardous Materials*, *137*(3), 1719-1728. https://doi.org/10.1016/j.jhazmat.2006.05.036

49. Gomez, V., Larrechi, M. S., & Callao, M. P. (2007). Kinetic and adsorption study of acid dye removal using activated carbon. *Chemosphere*, *69*(7), 1151-1158. https://doi.org/10.1016/j.chemosphere.2007.03.076

50. Lagergren, S. (1898). Zur theorie der sogenannten Adsorption geloster Stoffe. *Kungliga Svenska Vetenskapsakademiens Handlingar*, 24(4), 1-39.

51. Ho, Y. S., & McKay, G. (1999). Pseudo-second order model for sorption processes. *Process biochemistry*, *34*(5), 451-465. https://doi.org/10.1016/S0032-9592(98)00112-5

52. Crini, G., & Badot, P. M. (2008). Application of chitosan, a natural aminopolysaccharide, for dye removal from aqueous solutions by adsorption processes using batch studies: A review of recent literature. *Progress in Polymer Science*, *33*(4), 399-447. https://doi.org/10.1016/j.progpolymsci.2007.11.001

53. Aksu, Z. (2005). Application of biosorption for the removal of organic pollutants: A review. *Process biochemistry*, *40*(3-4), 997-1026. https://doi.org/10.1016/j.procbio.2004.04.008

54. Gong, R., Li, M., Yang, C., Sun, Y., & Chen, J. (2005). Removal of cationic dyes from aqueous solution by adsorption on peanut hull. *Journal of Hazardous Materials*, *121*(1-3), 247-250. https://doi.org/10.1016/j.jhazmat.2005.01.029

55. Ponnusami, V., Gunasekar, V., & Srivastava, S. N. (2009). Kinetics of methylene blue removal from aqueous solution using gulmohar (Delonix

regia) plant leaf powder: Multivariate regression analysis. *Journal of Hazardous Materials*, *169*(1-3), 119-127. https://doi.org/10.1016/j.jhazmat.2009.03.066

56. Ponnusami, V., Vikram, S., & Srivastava, S. N. (2008). Guava (Psidium guajava) leaf powder: novel adsorbent for removal of methylene blue from aqueous solutions. *Journal of Hazardous Materials*, *152*(1), 276-286. https://doi.org/10.1016/j.jhazmat.2007.06.107

57. Cheung, C. W., Porter, J. F., & Mckay, G. (2001). Sorption kinetic analysis for the removal of cadmium ions from effluents using bone char. *Water Research*, *35*(3), 605-612. https://doi.org/10.1016/S0043-1354(00)00306-7

58. Ayawei, N., Jnr, M. H., & Spiff, I. (2005). Rhizophora mangle waste as adsorbent for metal ions removal from aqueous solution. *European Journal of Scientific Research*, *9*(1), 21.

59. Shooto, N. D., Ayawei, N., Wankasi, D., Sikhwivhilu, L., & Dikio, E. D. (2016). Study on cobalt metal organic framework material as adsorbent for lead ions removal in aqueous solution. *Asian Journal of Chemistry*, *28*(2), 277-281. https://doi.org/10.14233/ajchem.2016.19202

60. Narin, I., Surme, Y., Soylak, M., & Dogan, M. (2006). Speciation of Cr (III) and Cr (VI) in environmental samples by solid phase extraction on Ambersorb 563 resin. *Journal of Hazardous Materials*, *136*(3), 579-584. https://doi.org/10.1016/j.jhazmat.2006.12.034

61. Fost, S. and Aly, M. (1981). *Adsorption Processes for Water Treatment*, Betterworth Publications.

62. Dąbrowski, A. (2001). Adsorption—from theory to practice. *Advances in Colloid and Interface Science*, *93*(1-3), 135-224. https://doi.org/10.1016/S0001-8686(00)00082-8

63. Ayawei, N., Angaye, S. S., Wankasi, D., & Dikio, E. D. (2015). Synthesis, characterization and application of Mg/Al layered double hydroxide for the degradation of congo red in aqueous solution. *Open Journal of Physical Chemistry*, *5*(3), 56-70. https://doi.org/10.4236/ojpc.2015.53007

64. Ayawei, N., Ekubo, A. T., Wankasi, D., & Dikio, E. D. (2015). Adsorption of congo red by Ni/Al-CO3: equilibrium, thermodynamic and kinetic studies. *Oriental Journal of Chemistry*, *31*(3), 1307. https://doi.org/10.13005/ojc/310307

65. Boparai, H. K., Joseph, M., & O'Carroll, D. M. (2011). Kinetics and thermodynamics of cadmium ion removal by adsorption onto nano zerovalent iron particles. *Journal of Hazardous Materials*, *186*(1), 458-465. https://doi.org/10.1016/j.jhazmat.2010.11.029

66. Noroozi, 5. 6. B., Sorial, G. A., Bahrami, H., & Arami, M. (2007). Equilibrium and kinetic adsorption study of a cationic dye by a natural

adsorbent—Silkworm pupa. *Journal of Hazardous Materials*, *139*(1), 167-174. https://doi.org/10.1016/j.jhazmat.2006.06.021

67. Hamdaoui, O. (2006). Batch study of liquid-phase adsorption of methylene blue using cedar sawdust and crushed brick. *Journal of Hazardous Materials*, *135*(1-3), 264-273. https://doi.org/10.1016/j.jhazmat.2005.11.062

68. Batzias, F. A., & Sidiras, D. K. (2004). Dye adsorption by calcium chloride treated beech sawdust in batch and fixed-bed systems. *Journal of Hazardous Materials*, *114*(1-3), 167-174. https://doi.org/10.1016/j.jhazmat.2004.08.014

69. Hameed, B. H., & El-Khaiary, M. I. (2008). Batch removal of malachite green from aqueous solutions by adsorption on oil palm trunk fibre: equilibrium isotherms and kinetic studies. *Journal of Hazardous Materials*, *154*(1-3), 237-244. https://doi.org/10.1016/j.jhazmat.2007.10.017

70. Hameed, B. H., & El-Khaiary, M. I. (2008). Sorption kinetics and isotherm studies of a cationic dye using agricultural waste: Broad bean peels. *Journal of Hazardous Materials*, *154*(1-3), 639-648. https://doi.org/10.1016/j.jhazmat.2007.10.081

71. Banerjee, S., & Dastidar, M. G. (2005). Use of jute processing wastes for treatment of wastewater contaminated with dye and other organics. *Bioresource technology*, *96*(17), 1919-1928. https://doi.org/10.1016/j.biortech.2005.01.039

72. Tran, H. N., You, S. J., Hosseini-Bandegharaei, A., & Chao, H. P. (2017). Mistakes and inconsistencies regarding adsorption of contaminants from aqueous solutions: A critical review. *Water Research*, *120*, 88-116. https://doi.org/10.1016/j.watres.2017.04.014

73. Saha, P., & Chowdhury, S. (2011). Insight into adsorption thermodynamics. *Thermodynamics*, *16*, 349-364. https://doi.org/10.5772/13474.